RSC Advances

ROYAL SOCIETY OF CHEMISTRY

PAPER

View Article Online
View Journal | View Issue

Cite this: *RSC Adv.*, 2020, **10**, 4710

Direct observation of dimethyl sulfide trapped by MOF proving efficient removal of sulfur impurities†

Masashi Morita, [ab] Akira Yonezu, [b] Shinpei Kusaka, [b] Akihiro Hori, [b] Yunsheng Ma [b] and Ryotaro Matsuda *[bc]

Received 20th November 2019
Accepted 14th January 2020

DOI: 10.1039/c9ra09702c

rsc.li/rsc-advances

Here, we report the adsorptive removal of trace amounts of dimethyl sulfide (DMS) using metal–organic frameworks (MOFs). Cu^{2+}-based MOFs with open metal sites (OMSs), $[Cu_3(btc)_2]$ (HKUST-1), where btc = 1,3,5-benzenetricarboxylate, and without OMSs, $[Cu_2(bdc)_2(dabco)]$ (Cu-JAST-1), where bdc = 1,4-benzenedicarboxylate and dabco = 1,4-diazabicyclo[2.2.2]octane, were investigated for the removal of DMS to compare their performance with that of Ag–Y zeolite, which is currently widely used in industry. HKUST-1 exhibited a considerably higher adsorption capacity for DMS than the other adsorbents, which was confirmed by breakthrough measurements. The adsorption state of DMS with HKUST-1 was directly revealed by single-crystal X-ray diffraction (SXRD) analysis and *in situ* Raman spectroscopy. In addition, it was shown that DMS can be removed by HKUST-1 even under humid conditions.

Introduction

The adsorptive removal of trace impurities using porous materials (*e.g.*, zeolites and activated carbon) is important for industry and environments.[1] Specifically, the removal of volatile organosulfur molecules is an important issue because these molecules are harmful to humans and toxic for various catalytic chemical reactions. Indeed, dimethyl sulfide (DMS), which damages steam reforming catalysts in fuel cell cogeneration systems, frequently contaminates natural gas used by cities (*i.e.*, city gas) worldwide. Currently, Ag–Y zeolite is widely utilized to remove several organosulfur molecules including DMS at ppm level concentrations from city gas at ambient temperatures.[2–4] However, for industrial use, Ag–Y zeolite is not efficient at removing trace amounts of toxic substances (*e.g.*, organosulfur molecules) because of its low adsorption capacity due to the limited silver content and the high cost of silver. Metal–organic frameworks (MOFs), which are constructed with metal ions and organic ligands, are perceived as next-generation adsorbents owing to their wide variety of structures and pore functions.[5–7] Of note, MOFs can bear coordinatively unsaturated metal ions that are called open metal sites (OMSs) and can strongly interact with guest molecules. Although there are several reports describing the removal of sulfur molecules using MOFs with OMSs, direct structural and spectroscopic evidence that explains the mechanism of desulfurization by these MOFs has not been shown.[8–11] HKUST-1, which is one of the representative MOFs with OMSs that are based on Cu^{2+} paddlewheel units, showed high catalytic, adsorption and separation properties.[12–14] However, the mechanism of its high performance as a porous material has not been sufficiently clarified.[15–19]

Herein, we investigated the ability of HKUST-1 (as a MOF with OMSs) (Fig. S1†) and Cu-JAST-1 (as a MOF without OMSs) (Fig. S2†) to remove trace amounts of DMS compared with that of Ag–Y zeolite. It is determined that OMSs in HKUST-1 can strongly trap DMS, which was directly proven by *in situ* SXRD and Raman measurements.

Experimental section

The general procedures of the experiments can be found in ESI.†

DMS breakthrough measurements

Breakthrough measurements were conducted at 303 K in a fixed-bed flow reactor (7 mm inner diameter) to which 1.1 g of each sample was added (Fig. S3†). The sample was heated at 393 K for 12 h under an N_2 flow to obtain a degassed sample. Then, DMS (2.3 vol%) balanced by Ar was flowed to the sample at a linear velocity of 0.003 m s^{-1} (7.3 sccm). The sulfur concentration in the inlet and outlet was monitored by a sulfur chemiluminescence detector (SCD, TS-2100 V, Mitsubishi Chemical Analytech Co.). The relative concentration (C/C_0) was

[a]Technology Innovation Division, Panasonic Corporation, 3-1-1 Yagumo-naka-machi, Moriguchi City, Osaka 570-8501, Japan
[b]Department of Chemistry and Biotechnology, School of Engineering, Nagoya University, Chikusa-ku, Nagoya 464-8603, Japan. E-mail: ryotaro.matsuda@chembio.nagoya-u.ac.jp
[c]Institute for Advanced Research, Nagoya University, Chikusa-ku, Nagoya 464-8603, Japan

† Electronic supplementary information (ESI) available: General procedures, characterization data, sorption data, Raman spectroscopy data and SXRD refinement data. CCDC 1950114–1950116. For ESI and crystallographic data in CIF or other electronic format see DOI: 10.1039/c9ra09702c

calculated from the sulfur concentration ratio of inlet and outlet. The sulfur adsorption capacity was calculated from the breakthrough time at the moment of the first detection of the relative concentration ($C/C_0 > 0.1$) in the outlet using eqn (1). The recyclability of HKUST-1 (0.2 g) was repeatedly tested using the same procedures. After the removal of guest molecules by heating at 393 K, the gas mixture of CH_4 (49.7 vol%), Ar (49.3 vol%) and trace amounts of DMS (1.0 vol%) was flowed into the fixed-bed flow reactor (7.3 sccm) at 303 K.

$$\text{Sulfur adsorption capacity(wt\%)} = \frac{\text{flow gas rate (sccm)} \times \text{inlet } C_0 \times \text{breakthrough time} \times 32}{22\,400 \times \text{weight}_{\text{adsorbents}}} \times 100 \tag{1}$$

SXRD analysis of DMS-adsorbed HKUST-1

A single crystal of HKUST-1 was placed in a capillary tube (0.4 mm diameter), which was heated under dynamic vacuum at 120 °C for 12 h to remove guest solvent molecules. Then, DMS (2.3 vol%) balanced by Ar was added to the capillary at 90 kPa, and the capillary remained at these conditions for 12 h to achieve equilibration. Then, the capillary tube was sealed. The SXRD measurement was performed at 203 K with a Rigaku XtaLab P200 diffractometer and a Dectris Pilatus 200 K CCD system equipped with a MicroMax-007 HF/VariMax rotating anode X-ray generator with confocal monochromated MoKα radiation. The crystal structure was determined by the direct method and refined by full-matrix least-squares refinement using SHELXL 2014/7. The uncoordinated guest and solvent molecules were omitted using the solvent mask of the Olex2 software.

Coincident *in situ* DMS adsorption/Raman spectroscopy

Raman spectroscopy was performed in a back-scattering geometry at room temperature using LabRAM HR Evolution (HORIBA). A laser with a 532 nm wavelength was used as an excitation source. Scattered light was detected using a Jobin-Yvon Raman microscope LabRAM HR Evolution and a Jobin-Yvon DU970P-UV-328 CCD (charge-coupled device) system. The sample was placed in the flow cell with a quartz window to conduct Raman measurement. After the cell was heated at 393 K, the gas mixture of CH_4 (56.5 vol%), Ar (42.5 vol%) and trace amounts of DMS (1.0 vol%) was flowed into the sample cell for the designated periods of times with and without H_2O at room temperature and Raman spectrum was measured.

Results and discussion

Synthesis and structural characterization

Powder X-ray diffraction (PXRD) patterns of HKUST-1, Cu-JAST-1 and Ag–Y zeolite were in good agreement with the reported patterns (Fig. S4–S6†).[2,20,21] The Brunauer–Emmett–Teller (BET) surface areas for HKUST-1, Cu-JAST-1 and Ag–Y zeolite were calculated to be 1681, 1809 and 717 $m^2 g^{-1}$, respectively, on the basis of the adsorption isotherms of N_2 at 77 K (Fig. S7†). These results were similar to previously reported values for these samples.[4,20,21] The BET surface area of Ag–Y zeolite was reduced by 20% after the Ag^+ ion exchange, which corresponds to a change in the chemical formula (Na–Y zeolite: 902 $m^2 g^{-1}$, Fig. S7†).

Separation of DMS from the gas mixture

Breakthrough curve measurements for HKUST-1, Cu-JAST-1 and Ag–Y zeolite were conducted to investigate the affinity to DMS and the adsorption capacity of each compound (Fig. 1). A curve with a small slope of Ag–Y zeolite was observed compared with those for the other samples, which implies that the diffusion of DMS in HKUST-1 and Cu-JAST-1 is smoother than that of Ag–Y zeolite owing to its narrow path in the supercage that contains Ag^+.[22] The DMS breakthrough times of Cu-JAST-1, Ag–Y zeolite and HKUST-1 were found to be 1.9, 6.5 and 14.8 h, respectively. On the basis of these breakthrough times, the adsorption capacities for DMS by Cu-JAST-1, Ag–Y zeolite and HKUST-1 were estimated to be 2.2, 7.2 and 17.0 wt%, respectively, which indicates that HKUST-1 has a 2.4 and 7.7 times higher capacity than Ag–Y zeolite and Cu-JAST-1, respectively. HKUST-1 exhibited a higher capacity than Cu-JAST-1, although Cu-JAST-1 has higher BET surface area than HKUST-1, which indicates that Cu-OMSs in HKUST-1 are essential for obtaining the high performance of DMS trapping. Furthermore, it is determined that the number of DMS molecules adsorbed in HKUST-1 is consistent with that of Cu-OMSs (S/Cu = 1.1), which suggests that DMS was trapped by Cu-OMSs in a Langmuir adsorption manner. In addition, PXRD pattern of HKUST-1 after DMS breakthrough measurement was in good agreement with that of degassed phase. This suggests that the structure of HKUST-1 was maintained even after DMS breakthrough measurements (Fig. S4d†). To investigate the recyclability with HKUST-1, we carried out DMS breakthrough measurements 3 cycles with a simulated real gas containing CH_4 (Fig. S8†). The DMS breakthrough times of first, second and third cycles were found to be 4.4, 4.6 and 4.1 h, respectively, and the adsorption

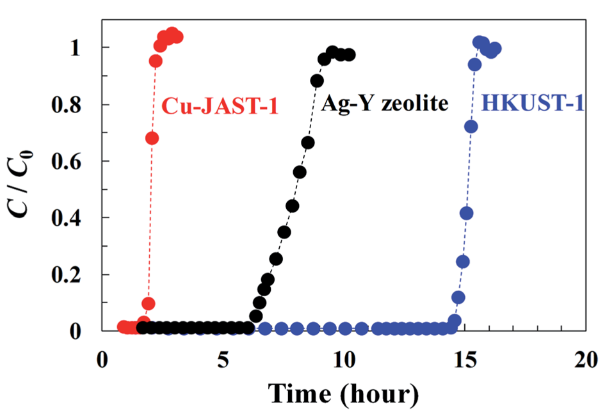

Fig. 1 Breakthrough curves of sulfur concentration for the DMS adsorption on HKUST-1, Cu-JAST-1 and Ag–Y-zeolite at 303 K.

capacities for DMS of each cycle were estimated to be 14.1, 14.3 and 13.9 wt%, respectively (Fig. 2). The DMS adsorption capacity was almost maintained after 3 cycles, indicating that the HKUST-1 is durable against the recycle use and efficiently trap DMS under the simulated real gas condition.

Direct observation of HKUST-1 with DMS adsorbed on OMSs by SXRD analysis

To elucidate the adsorptive mechanism at the molecular level, single-crystal X-ray diffraction (SXRD) measurement of a HKUST-1 crystal sealed in a glass capillary filled with a DMS vapor was conducted at 203 K (Fig. 3, S9 and Table S1†). It was observed that DMS molecules with the occupancy of 0.93 (=DMS/Cu) were clearly trapped on Cu-OMSs. The S atom of DMS exists just above Cu-OMSs. The Cu–S distance (2.55 Å) was much shorter than that of the sum of van der Waals radii (4.27 Å),[23] which is indicative of a coordination bond between S and Cu. The Cu–S–CH_3 angle was 101° and the –CH_3 groups were located above the oxygen atoms of carboxylate groups, which provided additional adsorption interactions.[24]

In situ DMS adsorption/Raman spectroscopy

The progress of DMS trapping on Cu-OMSs was monitored by *in situ* Raman spectroscopy. Fig. 4 presents the spectra for as-synthesized, degassed and DMS-adsorbed samples at different conditions. In the spectrum of as-synthesized HKUST-1, the peaks at 170 and 280 cm^{-1}, were observed, which are assignable to the vibrations of Cu–Cu and Cu–OH_2 in the paddle wheel unit with water molecules coordinated to OMSs, respectively (Fig. 4a).[25] After the removal of water by heating, the peak of the Cu–OH_2 vibration disappeared, and the peak of the Cu–Cu vibration was shifted to the higher energy region at 230 cm^{-1} (Fig. 4b). These results are consistent with the structural changes determined by SXRD, *i.e.*, shortening of the Cu–Cu distance from 2.62 to 2.49 Å (Table S1, Fig. S10–S12†). Then, the gas mixture of CH_4, Ar and DMS as a simulated real gas was flowed to the degassed sample at 303 K. After 15 min of flow, the Raman spectrum exhibited a new peak at 690 cm^{-1}, which is assignable to the C–S vibration (Fig. 4c).[26] At the same time, the peak of Cu–Cu vibration of degassed phase at 230 cm^{-1} decreased and that of the adsorbed phase appeared at 170 cm^{-1}. The Cu–Cu vibration peak of DMS-adsorbed HKUST-1 was observed at the same frequency as that of the as-synthesized HKUST-1, which correlates with the SXRD structures of these two phases that show the same Cu–Cu distance (Table S1, Fig. 3, S9, S10 and S12†). When the flowing time was increased from 15 to 60 min (Fig. 4d), the peak of the Cu–Cu vibration (230 cm^{-1}) further decreased and the peak of C–S vibration (690 cm^{-1}) increased. Furthermore, the peak of Cu–S vibration (285 cm^{-1}) appeared, and that of Cu–O vibration (500 cm^{-1}) increased owing to the structural symmetry change of paddle wheel unit upon DMS coordination. In addition, the spectrum was consistent with that observed in the absence of CH_4, which indicates that HKUST-1 selectively adsorbs DMS from a simulated real gas (Fig. 4e).

However, in the spectrum of Cu-JAST-1, the peak of the Cu–Cu vibration at 180 cm^{-1}, which was observed in the as-

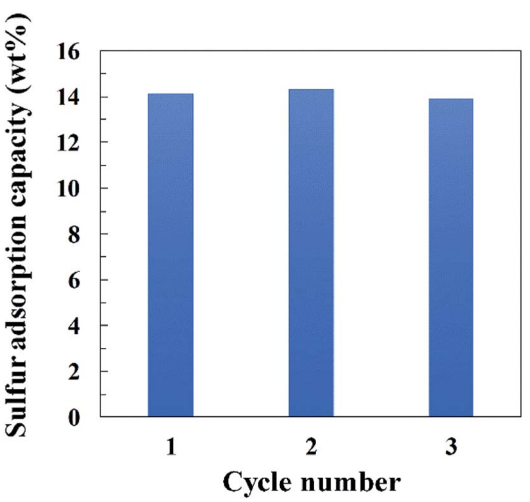

Fig. 2 Recyclability tests of HKUST-1 for sulfur adsorption capacity with the flowed gas mixture of CH_4 (49.7 vol%), Ar (49.3 vol%) and DMS (1.0 vol%) at 303 K.

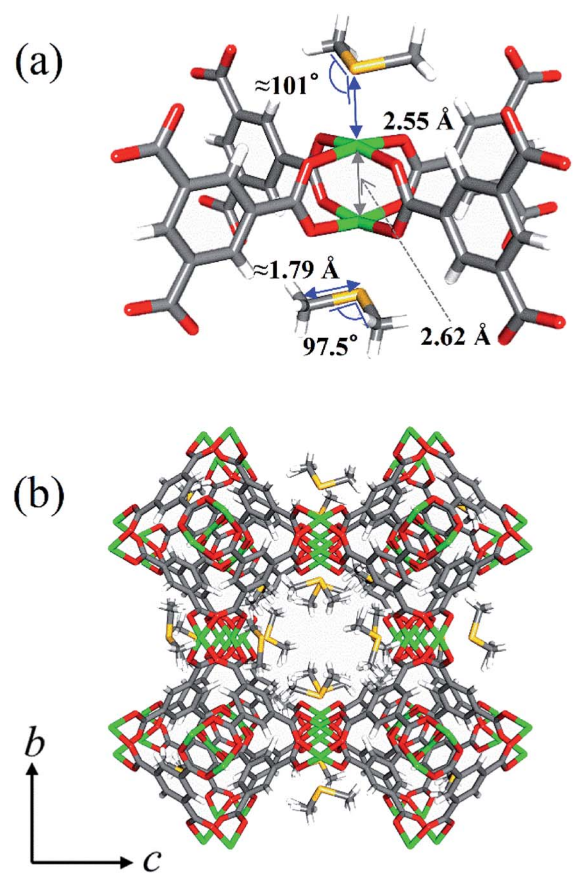

Fig. 3 Crystal structures of DMS-adsorbed HKUST-1. (a) Local paddle wheel structure with adsorbed DMS. (b) View of packing structure with DMS. Atoms are colored as follows: Cu, green; O, red; C, gray; H, white; S, yellow.

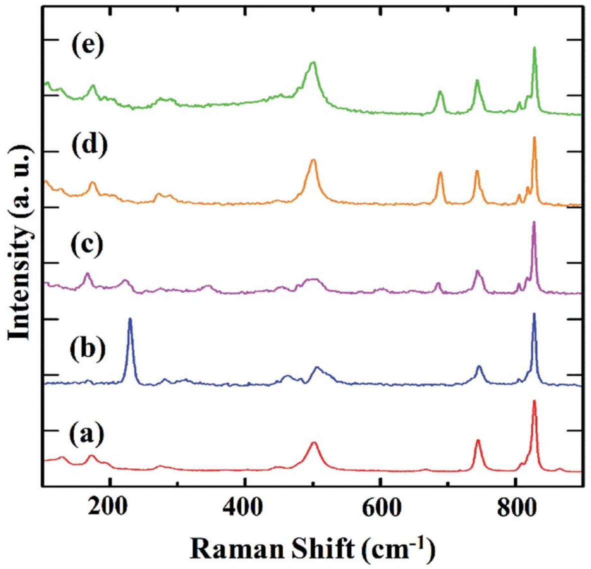

Fig. 4 Raman spectra of HKUST-1 with the flowed gas mixture of CH_4 (56.5 vol%), Ar (42.5 vol%) and DMS (1.0 vol%): (a) as-synthesized, (b) degassed, (c) flowing for 15 min, (d) flowing for 60 min and (e) flowing DMS (2.3 vol%) balanced by Ar.

synthesized sample, remained unchanged even after the removal of guest solvents and adsorption of DMS. This suggests that DMS molecules were not coordinated to Cu ions (Fig. S13†).

To test whether HKUST-1 can adsorb DMS under humid condition, we performed the same measurement using the simulated real gas with the typical humidity present in industrial gases (0.4 vol% H_2O) (Fig. S14†). The peaks of Cu–Cu (170 cm^{-1}) and Cu–S (285 cm^{-1}) vibrations appeared and those of C–S (690 cm^{-1}) and Cu–O (500 cm^{-1}) vibrations clearly increased for degassed and 15 and 30 min gas-flowed samples in the same way as dry gas. The result indicates that DMS has stronger interactions with Cu-OMSs than H_2O and can be effectively adsorbed by HKUST-1.

Conclusions

In summary, we evaluated the adsorption of trace amounts of DMS by Cu-OMSs MOF, HKUST-1. HKUST-1 exhibited higher sulfur adsorption than Cu-JAST-1, which had larger BET specific surface area but no OMSs. The results indicate that Cu-OMSs were effective for DMS adsorption. At the same time, HKUST-1 has higher DMS adsorption capacity than Ag-Y zeolite, which confirms its practical adsorption capacity. In addition, we performed direct observations using *in situ* SXRD and Raman spectroscopy measurements and experimentally revealed that DMS adsorbs to OMSs in HKUST-1. Furthermore, it was confirmed that Cu-OMSs in HKUST-1 selectively adsorb DMS from a simulated real gas even in the presence of moisture. This result is important for the practical industrial and environmental application of removing trace amounts of organosulfur molecules and serves as a guide for the future development of MOFs.

Conflicts of interest

There are no conflicts to declare.

Acknowledgements

This work was supported by the PRESTO (Grant No. JPMJPR141C) and CREST (Grant No. JPMJCR17I3) of the Japan Science and Technology Agency (JST), and JSPS KAKENHI grant numbers JP16H06032, JP17H03122, JP18K14043, JP18K05145, and JP19H02734.

Notes and references

1 S. U. Rege, R. T. Yang and M. A. Buzanowski, *Chem. Eng. Sci.*, 2000, **55**, 4827–4838.
2 S. Satokawa, Y. Kobayashi and H. Fujiki, *Appl. Catal., B*, 2005, **56**, 51–56.
3 K. Shimizu, N. Kobayashi, A. Satsuma, T. Kojima and S. Satokawa, *J. Phys. Chem. B*, 2006, **110**, 22570–22576.
4 D. Lee, E. Y. Ko, H. C. Lee, S. Kim and E. D. Park, *Appl. Catal., A*, 2008, **334**, 129–136.
5 S. Kitagawa, R. Kitaura and S.-I. Noro, *Angew. Chem., Int. Ed.*, 2004, **43**, 2334–2375.
6 D. Zhao, D. J. Timmons, D. Yuan and H. C. Zhou, *Acc. Chem. Res.*, 2011, **44**, 123–133.
7 H. Furukawa, K. E. Cordova, M. O'Keeffe and O. M. Yaghi, *Science*, 2013, **341**, 974.
8 M. Woellner, S. Hausdorf, N. Klein, P. Mueller, M. W. Smith and S. Kaskel, *Adv. Mater.*, 2018, **30**, 1704679.
9 C. Petit, B. Mendoza and T. J. Bandosz, *ChemPhysChem*, 2010, **11**, 3678–3684.
10 M. Savage, Y. Cheng, T. L. Easun, J. E. Eyley, S. P. Argent, M. R. Warren, W. Lewis, C. Murray, C. C. Tang, M. D. Frogley, G. Cinque, J. Sun, S. Rudić, R. T. Murden, M. J. Benham, A. N. Fitch, A. J. Blake, A. J. Ramirez-Cuesta, S. Yang and M. Schröder, *Adv. Mater.*, 2016, **28**, 8705–8711.
11 M. Morita, H. Wakita, T. Nomura, M. Higuchi and S. Kitagawa, *Microporous Mesoporous Mater.*, 2017, **243**, 351–354.
12 R. J. Kuppler, D. J. Timmons, Q. R. Fang, J. R. Li, T. A. Maskal, M. D. Young, D. Yuan, D. Zhao, W. Zhuang and H. C. Zhou, *Coord. Chem. Rev.*, 2009, **253**, 3042–3066.
13 B. Li, M. Chrzanowski, Y. Zhang and S. Ma, *Coord. Chem. Rev.*, 2016, **306**, 107–129.
14 L. Zhu, X. Q. Liu, H. L. Jiang and L. B. Sun, *Chem. Rev.*, 2017, **117**, 8129–8176.
15 C. Y. Sun, S. X. Liu, D. D. Liang, K. Z. Shao, Y. H. Ren and Z. M. Su, *J. Am. Chem. Soc.*, 2009, **131**, 1883–1888.
16 S. Xiang, W. Zhou, J. M. Gallegos, Y. Liu and B. Chen, *J. Am. Chem. Soc.*, 2009, **131**, 12415–12419.
17 J. Song, Z. Luo, D. K. Britt, H. Furukawa, O. M. Yaghi, K. I. Hardcastle and C. L. Hill, *J. Am. Chem. Soc.*, 2011, **133**, 16839–16846.
18 S. C. McKellar, A. J. Graham, D. R. Allan, M. I. H. Mohideen, R. E. Morris and S. A. Moggach, *Nanoscale*, 2014, **6**, 4163–4173.

19 V. K. Peterson, P. D. Southon, G. J. Halder, D. J. Price, J. J. Bevitt and C. J. Kepert, *Chem. Mater.*, 2014, **26**, 4712–4723.

20 S. S.-Y. Chui, S. M.-F. Lo, J. P. H. Charmant, A. G. Orpen and I. D. Williams, *Science*, 1999, **283**, 1148–1150.

21 R. Matsuda, W. Kosaka, R. Kitaura, Y. Kubota, M. Takata and S. Kitagawa, *Microporous Mesoporous Mater.*, 2014, **189**, 83–90.

22 A. Gedeon, D. E. Favre, D. Reichert, J. MacNeil and B. F. Chmelka, *J. Phys. Chem. A*, 1999, **103**, 6691–6703.

23 S. Alvarez, *Dalton Trans.*, 2013, **42**, 8617–8636.

24 Y. Hijikata and S. Sakaki, *Inorg. Chem.*, 2014, **53**, 2417–2426.

25 M. Todaro, A. Alessi, L. Sciortino, S. Agnello, M. Cannas, F. M. Gelardi and G. Buscarino, *J. Spectrosc.*, 2016, **2016**, 1–7.

26 M. M. El-Etri and W. M. Scovell, *Inorg. Chim. Acta*, 1991, **187**, 201–206.